ELSEVIER

Contents lists available at ScienceDirect

Journal of Controlled Release

journal homepage: www.elsevier.com/locate/jconrel





Hepatocyte-targeted delivery of imiquimod reduces hepatitis B virus surface antigen

Nojoud AL Fayez^{a,d}, Elham Rouhollahi^a, Chun Yat Ong^a, Jiamin Wu^a, Anne Nguyen^a, Roland Böttger^a, Pieter R. Cullis^{b,c}, Dominik Witzigmann^{b,c}, Shyh-Dar Li^{a,c,*}

- ^a Faculty of Pharmaceutical Sciences, University of British Columbia, Vancouver, British Columbia V6T 1Z3, Canada
- b Department of Biochemistry and Molecular Biology, University of British Columbia, Vancouver, British Columbia V6T 1Z3, Canada
- NanoMedicines Innovation Network (NMIN), University of British Columbia, Vancouver, British Columbia V6T 1Z3, Canada
- ^d King Abdulaziz City for Science and Technology, Riyadh, Saudi Arabia

ARTICLE INFO

Keywords: Phospholipid-free small unilamellar vesicles (PFSUVs) Imiquimod (IMQ) Hepatitis B virus (HBV) Chronic hepatitis B (CHB) Hepatitis B surface antigen (HBsAg) Interferon-α (IFN-α)

ABSTRACT

Hepatitis B virus (HBV) can rapidly replicate in the hepatocytes after transmission, leading to chronic hepatitis, liver cirrhosis and eventually hepatocellular carcinoma. Interferon-α (IFN-α) is included in the standard treatment for chronic hepatitis B (CHB). However, this therapy causes serious side effects. Delivering IFN-α selectively to the liver may enhance its efficacy and safety. Imiquimod (IMQ), a Toll-Like Receptor (TLR) 7 agonist, stimulates the release of IFN-α that exhibits potent antiviral activity. However, the poor solubility and tissue selectivity of IMQ limits its clinical use. Here, we demonstrated the use of lipid-based nanoparticles (LNPs) to deliver IMQ and increase the production of IFN- α in the liver. We encapsulated IMQ in two liver-targeted LNP formulations: phospholipid-free small unilamellar vesicles (PFSUVs) and DSPG-liposomes targeting the hepatocytes and the Kupffer cells, respectively. In vitro drug release/retention, in vivo pharmacokinetics, intrahepatic distribution, IFN-α production, and suppression of serum HBV surface antigen (HBsAg) were evaluated and compared for these two formulations. PFSUVs provided >95% encapsulation efficiency for IMQ at a drug-to-lipid ratio (D/L) of 1/20 (w/w) and displayed stable drug retention in the presence of serum. DSPG-IMQ showed 79% encapsulation of IMQ at 1/20 (D/L) and exhibited $\sim 30\%$ burst release when incubated with serum. Within the liver, PFSUVs showed high selectivity for the hepatocytes while DSPG-liposomes targeted the Kupffer cells. Finally, in an experimental HBV mouse model, PFSUVs significantly reduced serum levels of HBsAg by 12-, 6.3and 2.2-fold compared to the control, IFN-a, and DSPG-IMQ groups, respectively. The results suggest that the hepatocyte-targeted PFSUVs loaded with IMQ exhibit significant potential for enhancing therapy of CHB.

1. Introduction

Chronic hepatitis B (CHB) caused by Hepatitis B viral (HBV) infection is one of the leading causes for severe liver diseases and liver transplantation worldwide [1]. According to the World Health Organization (WHO), approximately 300 million people are currently living with CHB with an estimate rise of a cumulative 20 million deaths between 2015 and 2030, if not treated [2]. CHB is an unmet global health challenge. The standard of care for CHB includes nucleoside analogues to block the viral replication and interferon (IFN) that enhances the cell immunity against HBV. However, these drugs are not curative, and in particular, IFN therapy is not well tolerated by most patients due to its systemic side effects [3]. According to the monograph of REBIF® (IFN, Serono Canada

Inc), >50% patients experience injection site inflammation, influenzalike symptoms, headache and rhinitis. To reduce the toxicity and enhance the efficacy, an alternative approach is to induce release of endogenous IFN locally in the liver.

One of the best studied immune receptors that involve activation of the innate immune system, are the Toll-Like Receptors (TLRs). TLRs recognize highly conserved motifs found in bacteria, viruses and fungi, inducing immune responses against these invaders [4]. Activation of some subtypes of TLRs, such as TLR3, 4, 7 and 9, by their agonists is associated with production of IFNs [5]. In a HBV-hepatocyte cell culture model, resiquimod, a TLR7/8 agonist, was shown to induce interferon- α release and down-regulate HBV transcription and antigen production [6,7]. A phase IIa clinical study for chronic hepatitis C (CHC) therapy

^{*} Corresponding author at: Faculty of Pharmaceutical Sciences, University of British Columbia, Vancouver, British Columbia V6T 1Z3, Canada. E-mail address: shyh-dar.li@ubc.ca (S.-D. Li).

displayed a reduction in viral levels when resiquimod was administered orally at 0.02 mg/kg. However, this treatment caused significant systemic immune activation that led to trial withdrawal. The results support the hypothesis that efficacy and safety of this type of treatment would be improved if a TLR agonist can be targeted to the hepatocytes with limited systemic exposure.

In this study, we compared efficacy of two types of liver-targeted lipid nanoparticle (LNP) formulations loaded with a TLR 7 agonist, including DSPG-liposomes [8] and phospholipid-free small unilamellar vesicles (PFSUVs) [9] for targeting two different types of cells in the liver, the Kupffer cell and hepatocyte, respectively. The DSPG-liposome formulation (DSPC, Chol and DSPG; 53:26:21, molar ratio) was adopted from the AmBisome formulation that has been demonstrated to target the Kupffer cells [8]. PFSUVs composed of cholesterol and Tween80 (5:1 molar ratio) were developed by our group, displaying predominant accumulation in the hepatocytes after IV administration [9–11].

We selected a TLR7 agonist, imiquimod (IMQ), for this study based on the following reasons: First, IMQ has been clinically approved with established pharmacology and safety profiles [12]. It is formulated in a topical cream for treating Human Papillomavirus (HPV)-infected genital warts with clinically established antiviral efficacy. Second, IMQ is a pure agonist for TLR7 that can lead to IFN- α release, the major antiviral molecule [13], while resiquimod also activates TLR8 that is responsible for the production of other pro-inflammatory cytokines that might induce additional side effects [14]. Moreover, IMQ is insoluble in water or any injectable organic solvents such as ethanol, and its systemic delivery requires advanced technologies, such as LNPs.

We fabricated these two types of LNPs and actively loaded IMQ into them. We then examined whether these two formulations could stably retain IMQ in the presence of serum. Their pharmacokinetics, liver uptake and IFN- α production profiles were compared in mice. Finally, we conducted an *in vivo* study in an experimental mouse model expressing HBV surface antigen (HBsAg) and compared their efficacy in inducing IFN- α in the liver to suppress HBsAg production.

2. Materials and methods

2.1. Materials

HepG2 cells were provided kindly by Dr. Thomas Chang (Faculty of Pharmaceutical Sciences at UBC, Vancouver, Canada). HBsAg plasmid was a gift from Wang-Shick Ryu (Addgene plasmid # 103013). Alexa Fluor® 488 Phalloidin and mouse IFN-α ELISA Kit were purchased from Thermo Fisher Scientific (Waltham, MA, USA). DiR (DilC $_{18}$ (7);1,1'-Dioctadecyl-3,3,3',3'-Tetramethylindotricarbocyanine Iodide) was purchased from Biotium Inc. (Fermont, CA, USA). Dialysis membrane (10 kDa molecular weight cut-off, MWCO) was purchased from Spectrum Labs (Waltham, MA, USA). Recombinant Mouse IFNAA Protein was purchased from R&D Systems Inc., (Minneapolis, MN, USA) All other organic solvents, reagents and buffers were of analytical grade and obtained from Sigma Aldrich (Oakville, ON, Canada).

2.2. Lipid nanoparticle (LNP) preparation and characterization

PFSUVs containing cholesterol (Chol) and TWEEN80 were prepared as previously described [9]. Chol and TWEEN80 (5:1 molar ratio) were dissolved in ethanol (10 mg total lipid/mL) and mixed with 250 mM ammonium sulfate at a flow ratio of 1:3 and a total flow rate of 15 mL/min at the room temperature using NanoAssemblr Benchtop (Precision Nanosystems, Vancouver, BC, Canada). The particles were collected and dialyzed overnight against 100 mM sodium acetate buffer (pH 5) to remove ethanol. PFSUVs were further concentrated to 25 mg lipid/mL using a tangential flow filtration (TFF) system (KrosFlo KR2i, Spectrum Laboratories, Rancho Dominguez, CA, USA) operating in the ultrafiltration mode and filtered through a diafiltration cartridge with a MWCO of 500 kDa (MidiKros Hollow Fiber Filter, surface area 115 cm², fiber

inner diameter 0.5 mm, length 20 cm, Spectrum Laboratories) at a flow rate of 40 mL/min.

DSPG-liposomes containing DSPC, Chol and DSPG (53:26:21, molar ratio) were fabricated by the thin film hydration method [8]. Briefly, lipid mixture was dissolved and mixed in chloroform and dried under vacuum using a rotary evaporator to form a thin lipid film. The thin film was hydrated with 250 mM ammonium sulfate at 30 mg lipids/mL and further extruded through 200, 100 and then 50 nm polycarbonate membranes using a Mini-Extruder (Avanti Polar Lipids, Alabaster, USA), followed by dialysis overnight against 100 mM sodium acetate buffer (pH 5).

For fluorescently labeled LNPs, DiR (lipophilic carbocyanine DiOC18 (7) dye) was included in the lipid formulations at 1.1 mol%. Particle size, polydispersity index (PDI) and zeta potential of the LNPs were measured by dynamic light scattering (DLS) using Zetasizer NanoZS (Malvern Instruments, Malvern, UK). DiR concentration was measured using a fluorescence microplate reader at Ex/Em wavelengths of 745/780 nm.

2.3. IMQ loading

IMQ was loaded into LNPs using the solvent-assisted active loading technology (SALT) [15]. IMQ was dissolved in DMSO and mixed with LNPs at various drug-to-lipid (D/L) ratios ranging from 1/20 to 1/5 (w/w), and the final DMSO content in the mixture was <10% (v/v). The mixture was incubated at 37 °C for 1 h and quenched on ice for 2 min. The formulation was further dialyzed against HEPES (4-(2-hydroxyethyl)-1-piperazineethanesulfonic acid) buffered saline (HBS, pH 7.4) over night. The encapsulation efficiency (EE) was determined using ultra performance liquid chromatography (UPLC) by comparing the D/L before and after dialysis. For UPLC measurement, 15 μ L of the LNPs was mixed with 45 μ L ethanol and sonicated for 5 min, followed by injection of 10 μ L of the sample for analysis.

2.4. Ultra performance liquid chromatography (UPLC)

IMQ concentration was measured using an ACQUITY UPLC H-Class System (Waters, Milford, MA, USA) coupled online to a photodiode array (PDA) detector (wavelength 320 nm) and a QDa mass spectrometer operated in positive ionization mode. A BEH-C18 column (inner diameter: 2.1 mm; length: 100 mm; particle size: 1.7 m, Waters) was used for separation, with a gradient mobile phase containing a mixture of eluent A and B (0.1% aqueous TFA and 0.1% TFA in methanol, respectively) at a flow rate of 0.3 mL/min. The gradient used was as follows: 0 min: A/B (95/5); 2 min: A/B (95/5); 8 min: A/B (0/100); 11 min: A/B (0/100); 11.1 min: A/B (95/5); 13 min: A/B (95/5). For mass spectrometry, the ionization was measured at 250 °C (source temperature) using a cone voltage of 65 V, and concentration of IMQ was determined by integrating the single ion recognition (SIR) peak for the singly charged molecular ion (m/z 241) acquired at a capillary voltage of 0.5 V. The same chromatographic method was used in conjunction with an evaporative light scattering (ELS) detector to determine lipid concentrations.

2.5. Cryogenic transmission electron microscopy (CryoTEM)

Empty LNPs and loaded IMQ-LNPs (25 mg lipid/mL) were deposited onto a glow-discharged copper grid, vitrified using a FEI Mark IV Vitrobot (FEI, Hillsboro, OR, USA), and imaged using a 200 kV Glacios microscope equipped with a Falcon III camera at the UBC High Resolution Macromolecular Cryo-Electron Microscopy facility (Vancouver, BC, Canada).

2.6. In vitro drug retention

LNPs loaded with IMQ (1.3 mg IMQ/mL) was mixed at a 1:4 ratio (ν /

v) with fetal bovine serum (FBS) (Gibco Laboratories, Gaithersburg, MD, USA) and incubated at 37 °C. After 10–120 min of incubation, the sample was collected and purified using size exclusion chromatography (SEC) on a Sephadex G-25 PD10 gel to separate the released drug. Fortyfive μL of the sample before and after SEC was mixed with 300 μL ethanol, vortexed for 30 s, placed on ice for 30 min, and centrifuged twice at 12,500 rpm for 5 min. The supernatant (280 μL) was collected, lyophilized, and reconstituted in 45 μL of ethanol. Ten μL of the sample was then injected into the UPLC for drug and lipid analysis as described above. Drug retention was calculated following Eq. (1), where (D/L)_i and (D/L)_f, are the initial and final drug-to-lipid ratio, respectively.

$$Drug \ retention = \frac{(D/L)_f}{(D/L)_i} \times 100\% \tag{1}$$

2.7. Animals

Female CD1 mice (18-20~g, 5-6 weeks old) were purchased from The Jackson Laboratory (Bar Harbor, ME). All the *in vivo* studies were conducted in accordance with an established protocol approved by the Animal Care Committee of the University of British Columbia (Vancouver, BC, Canada).

2.8. Pharmacokinetics

PFSUVs-IMQ and DSPG-IMQ were intravenously administered to CD-1 mice at 5 mg IMQ/kg (80-100 mg lipid/kg). Blood was collected at 0.083, 0.5, 1, 3, 6 and 24 h post injection and promptly transferred into an EDTA-coated tube. Plasma was separated by centrifugation for 10 min at 500 g at 4 °C. Mouse liver was collected after euthanasia and washed twice with PBS, blotted dry, and weighed (~ 0.2 g) into a 1.5 mL microtube (Next Advance, Inc., Troy, NY, USA). Protease inhibitor cocktail in PBS (1:100 v/v dilution, Sigma Aldrich) was added to the tissue (0.3 mL per 0.1 g tissue), and homogenized at 4 °C for 5 min using a tissue homogenizer Bullet blender (Next Advance, Inc., Troy, NY, USA) at an instrument speed of 10. The plasma and liver homogenate (45 μ L) was then subjected to the same UPLC and ELISA analyses for IMQ and IFN- α measurements, respectively, as described above. Positive control mice were injected subcutaneously (s.c.) with IFN-α at 30,000 IU (equivalent to 1.23 μg IFN- α) and subjected to the same IFN- α measurements in plasma and liver.

2.9. Intrahepatic distribution of LNPs

Particles labeled with DiR were injected intravenously into mice at a dose of $0.3~\mu g$ DiR/g. Mice were euthanized 2~h post injection and the liver was collected, washed with PBS and stored overnight in 10% formalin in PBS (v/v) at the room temperature. Liver sections with a thickness of 40 µm were produced using a vibratome instrument (Precisionary Instruments LLC, Boston, MA, USA) collected in PBS. The sections were incubated in 0.1% (v/v) Triton X-100 in PBS for 5 min, washed with PBS three times and subsequently incubated in 1% (v/v) bovine serum albumin in PBS for 10 min. After three PBS washes, the sections were incubated in Alexa Fluor® 488 Phalloidin (APh, 80 μL, 1 U/mL) for 30 min and further washed with PBS. The stained section was mounted on a glass slide with a drop of Fluoroshield® containing DAPI (Sigma Aldrich). Sections were imaged using a confocal microscope (Zeiss LSM 700) at 200× magnification and processed with ZEN software (both Carl Zeiss, Oberkochen, Germany). The hepatocytes and sinusoidal cells were identified by their nuclear morphology and phalloidin staining, and their association with DiR-LNPs was recorded.

2.10. In vivo efficacy

Mice were treated with $10~\mu g$ HBsAg plasmid using the hydrodynamic injection (HDI) technique to transiently transfect their

Table 1 Characterization of PFSUVs-IMQ prepared with different D/L ratios. Data = mean + SEM (n = 3).

D/L ratio (w/w)	Size (nm)	PDI	Encapsulation efficiency (%)	ξ potential (mV)
1/20	54.9 ± 0.7	0.126 ± 0.033	96.3 ± 6.4	-2.43 ± 0.76
1/10	57.2 ±	0.146 ± 0.020	55.3 ± 2.9	-1.20 ± 0.29
1/6.7	56.5 ±	0.095 ± 0.022	25.1 ± 3.0	-2.90 ± 0.48
1/5	68.0 ± 2.6	0.237 ± 0.026	15.7 ± 0.3	-4.98 ± 1.14

hepatocytes with HBsAg [16]. The plasmid DNA was dissolved in sterile saline in a volume equivalent to 8% body weight and injected into mice within 4-8 s via the tail vein. Mice were treated either with saline (negative control), IFN- α at 1.23 µg/mouse (positive control), PFSUVs-IMQ or DSPG-IMQ at 5 mg IMQ/kg (80-100 mg lipid/kg), 6 h post transfection. Body weight was monitored and blood was collected in EDTA-coated tubes at 6 h, 1 d, 2 d and 3 d after plasmid transfection. Plasma was separated by centrifugation for 10 min at 10,000 g at 4 °C, and HBsAg levels were quantified using the HBsAg (Hepatitis B surface antigen) ELISA Kit (Elabscience, Houston, TX, USA) according to manufacturer's protocol. Blood samples collected on day 3 were subjected to complete blood count (CBC), serum alanine aminotransferase (ALT) and aspartate aminotransferase (AST) measurements by IDEXX Reference Laboratories Ltd. (Delta, BC, Canada). Values were compared to the reference values provided by Charles River for CD-1 mice. Organs (heart, liver, lung, spleen and kidneys) were collected after euthanasia on day 3, washed with PBS, and stored in 10% (ν/ν) formalin in PBS for 48 h at the room temperature. Paraffin-embedded liver section, haematoxylin and eosin (H&E) staining, and microscopic imaging were performed by Wax-it Histology Services Inc. (Vancouver, BC, Canada). H&E histology images were examined by board certified pathologist Dr. Ian Walch at the University of British Columbia - Department of pathology and laboratory medicine.

2.11. Statistical analysis

All data are presented as mean \pm SEM. Statistical analysis was performed with GraphPad Prism version 8.0 (GraphPad Software, San Diego, CA, USA). Comparisons between groups were made by unpaired t-test and one way ANOVA. A difference with p < 0.05 was considered to be statistically significant.

3. Results and discussion

While type I IFNs are used clinically in the treatment of viral hepatitis such as CHB, they cause significant adverse events in majority of the patients [17,18]. Here, we explored an alternative approach to boost IFN- α production locally in the liver by liver-targeted delivery of IMQ, a TLR 7 agonist, to enhance the therapy and reduce the systemic exposure and toxicity. In this study, we also aimed to compare which type of liver-targeted LNPs was superior, including PFSUVs for hepatocyte targeting and DSPG-liposomes for Kupffer cell targeting. We first prepared and characterized PFSUVs-IMQ and DSPG-IMQ formulations.

3.1. Particles characterization

IMQ was actively loaded into PFSUVs via the ammonium sulfate gradient at a range of drug-to-lipid (D/L) ratios (1/20 to 1/5) in the presence of <10% DMSO. This technique (named SALT) developed by us has been shown to promote active loading of insoluble weak base compounds to the aqueous core of liposomes [15]. DMSO was used to increase the drug solubility and the lipid bilayer permeability,

Table 2 Characterization of LNP formulations loaded with IMQ prepared at a D/L of 1/20. Data = mean \pm SEM (n = 3).

D/L ratio (w/w)	Size (nm)	PDI	Encapsulation Efficiency (%)	ξ potential (mV)
PFSUVs	54.9 \pm	0.126 \pm	96.3 ± 6.4	-2.43 ± 0.76
	0.7	0.033		
DSPG -	86.7 \pm	$0.034~\pm$	79.6 ± 3.0	-28.50 ± 0.32
Liposome	0.8	0.001		

facilitating the drug permeation into the liposomal core [19]. DMSO was completely removed from the final formulation after dialysis [20]. As shown in Table 1 and Fig. S.1a (in the supplementary information), the

PFSUV particles displayed a comparable size of $\sim\!55$ nm and PDI $<\!0.2$ at D/L of 1/20, 1/10 and 1/6.7. However, the average size and PDI increased to $\sim\!70$ nm and >0.2, respectively, at a D/L of 1/5. The encapsulation efficiency (EE) of IMQ was $>\!95\%$ at a D/L of 1/20 as shown in in Table 1 and Fig. S.1b (in the supplementary information) and decreased as the D/L increased. This suggests that the loading capacity of IMQ reached the maximum at a D/L of 1/20. The data also indicate that loading a larger amount of IMQ (D/L = 1/5) into PFSUVs than the maximal loading capacity resulted in bigger and heterogeneous particles. Therefore, the formulation with a D/L of 1/20 was selected for further studies and compared to the DSPG-liposomal formulation, which was adopted from the AmBisome formulation that displays Kupffer cell targeting [21]. DSPG-liposomes were prepared using the thin-film

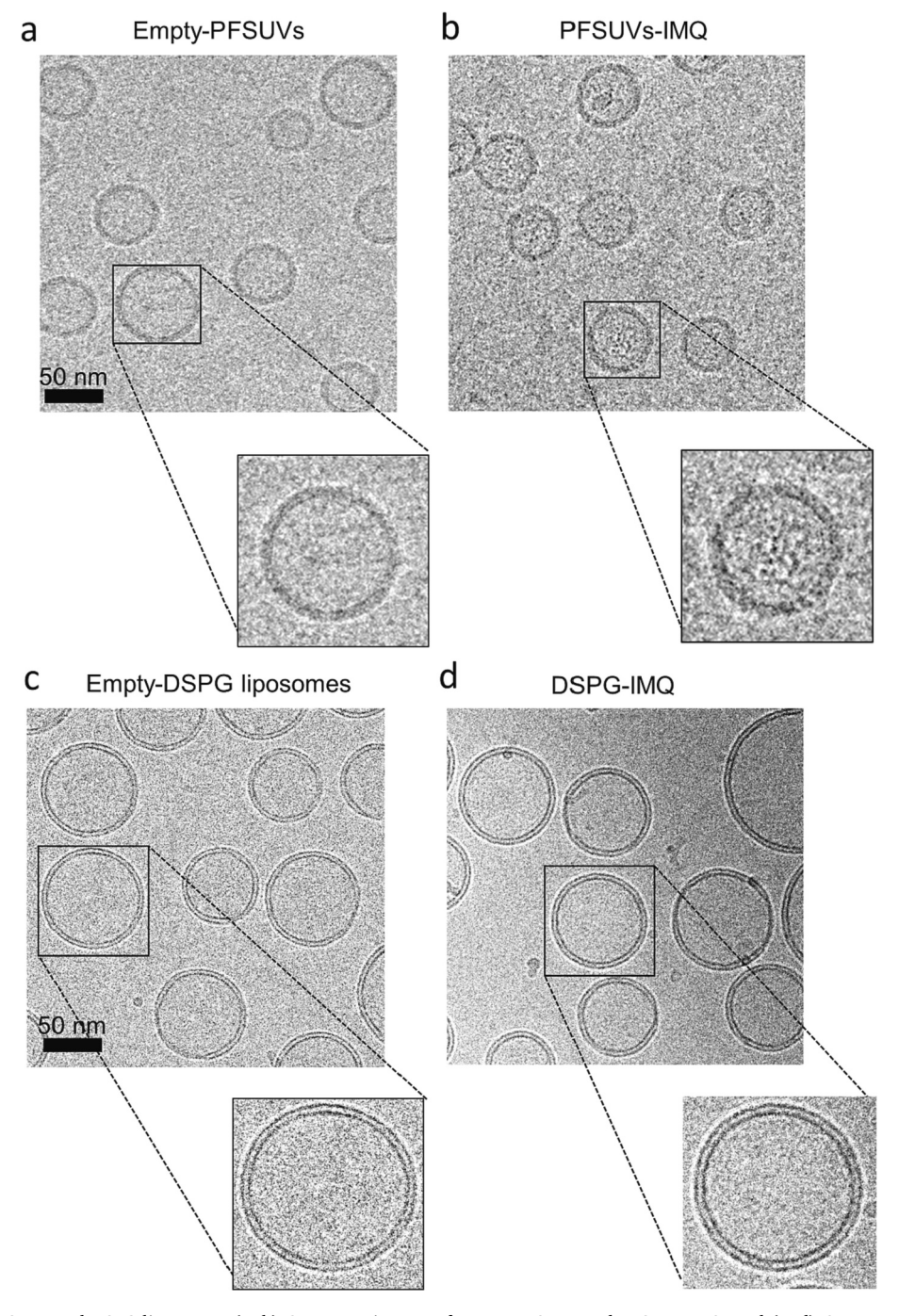


Fig. 1. Morphology of PFSUVs and DSPG-liposomes. (a, b) Cryo-TEM images of empty PFSUVs and PFSUVs-IMQ, and (c, d) Cryo-TEM images of empty DSPG-liposomes and DSPG-IMQ.

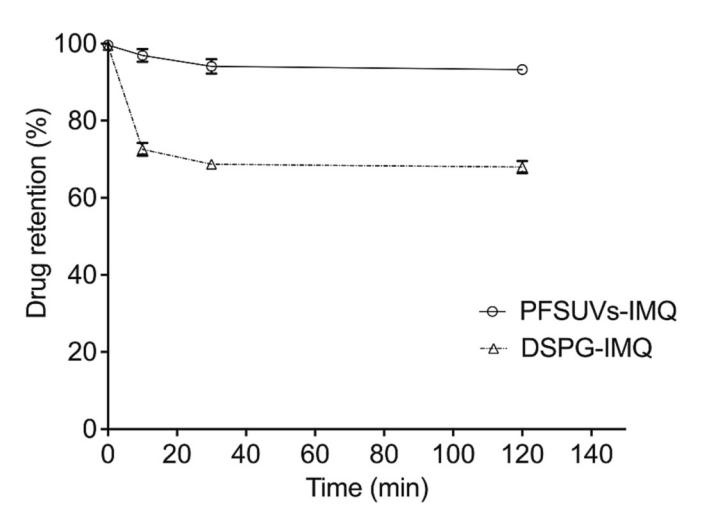


Fig. 2. In vitro drug retention of PFSUVs-IMQ and DSPG-IMQ in fetal bovine serum (FBS) at 37 $^{\circ}$ C. Data = mean \pm SEM (n=3).

hydration method, and IMQ was loaded using the SALT technique at a D/L of 1/20. As shown in Table 2, both formulations displayed homogenous particles with an average size of 55 and 87 nm for PFSUVs and DSPG-liposomes, respectively. PFSUVs encapsulated >95% of IMQ, whereas DSPG-liposomes exhibited $\sim80\%$ encapsulation efficiency (EE).

Morphological characteristics (size, lamellarity, drug loading) of the empty and IMQ loaded LNPs were analyzed using CryoTEM (Fig. 1). The particles displayed a spherical shape with sizes between 50 and 60 nm and 80–100 nm for PFSUVs and DSPG-liposomes, respectively, which were consistent with the DLS results. Electron-dense structures inside the PFSUVs-IMQ particles indicate that IMQ molecules were encapsulated in the aqueous core, while such structures were not identifiable in DSPG-IMQ. This could be due to that the EE was lower in DSPG-IMQ compared to PFSUVs-IMQ, suggesting an insufficient amount of IMQ molecules were loaded per DSPG particle to form electron-dense structures within the liposomes.

3.2. Drug retention

We conducted an *in vitro* drug retention study in serum to evaluate the ability of the LNP formulations to retain IMQ within the particles during plasma circulation before reaching the liver. PFSUVs-IMQ or DSPG-IMQ was incubated at 1:4 ratio (ν/ν) in FBS at 37 °C. Since both formulations have been shown to effectively accumulate in the liver within 2 h, we examined drug retention at 10, 30 and 120 min. At each

time point, samples were collected and purified via size exclusion chromatography (SEC) to remove released IMQ. The concentration of retained IMQ was measured using UPLC. PFSUVs showed stable IMQ retention over the period of 120 min with <10% drug leakage (Fig. 2). Conversely, a burst release (\sim 30%) from DSPG-IMQ was measured in 30 min, but then no more drug leakage for 2 h. The data indicate that PFSUVs were more stable in retaining IMQ in the presence of serum compared to DSPG-liposomes.

3.3. Pharmacokinetics

We then examined the pharmacokinetic profiles of the LNP-IMQ formulations. Free IMQ could not be introduced as a control because the drug is not soluble in water or any injectable solvent. LNP-IMQ was IV injected into female CD-1 mice at a dose of 5 mg IMQ/kg. Plasma and liver were collected at 0.083, 0.5, 1, 3, 6 and 24 h post administration and analyzed for IMQ concentration. The plasma profiles in Fig. 3a demonstrated rapid clearance of both LNP formulations. This is in-line with our previously reported data displaying rapid plasma clearance of PFSUVs with a half-life of <20 min [9]. The DSPG-liposomes also showed rapid eliminattion from the plasma after IV delivery [8]. Nevertheless, the plasma area under the curve (AUC) for DSPG-IMO was ~20-fold higher than that of PFSUVs-IMQ (Table 3). Both LNP formulations were found effectively accumulated in the liver (Fig. 3.b) with comparable AUC (Table 3). The AUC ratio between liver and plasma in PFSUVs-IMQ and DSPG-IMQ groups were 27.1 and 1.4, respectively (Table 3), and the AUC ratio (liver/plasma) for the PFSUVs-IMQ treated mice was ~20-fold increased. The data suggest PFSUVs were more effective in targeting IMQ to the liver compared to DSPG-liposomes, while both LNP formulations displayed significant liver homing ability.

3.4. Intrahepatic distribution

Although both LNPs formulations displayed efficient liver targeting, their delivery to different cell populations within the liver was distinct. We IV injected DiR-labeled PFSUVs or DSPG-liposomes at 0.3 µg DiR/g into female CD-1 mice and examined the intrahepatic distribution 2 h later. The liver was collected, sectioned, stained with DAPI for nuclei

Table 3 Area under the curve analysis of the pharmacokinetic profiles in Fig. 3. Data = mean \pm SEM (n = 3–5).

	PFSUVs-IMQ	DSPG-IMQ
AUC _{plasma} (μg*h/mL)	0.11 ± 0.02	2.46 ± 0.06
AUC Liver ($\mu g^*h/mL$)	2.91 ± 0.68	3.32 ± 0.18
AUC ratio (Liver:Plasma)	27.1	1.4

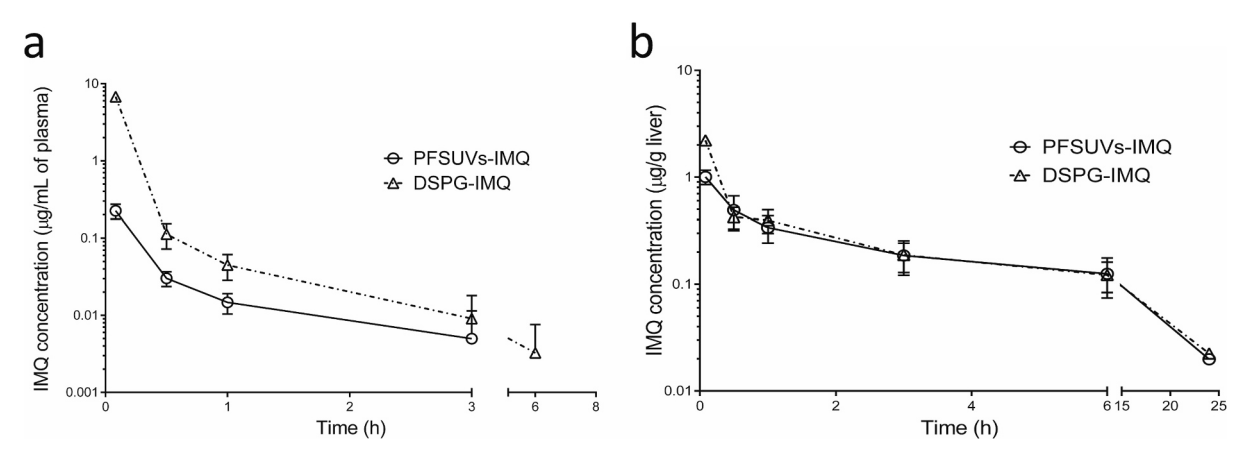


Fig. 3. Pharmacokinetic profiles of IV injected PFSUVs-IMQ and DSPG-IMQ in (a) plasma and (b) liver in female CD-1 mice after receiving a dose at 5 mg IMQ/kg. Data = mean \pm SEM (n = 3–5). SEM bars are within some data symbols.

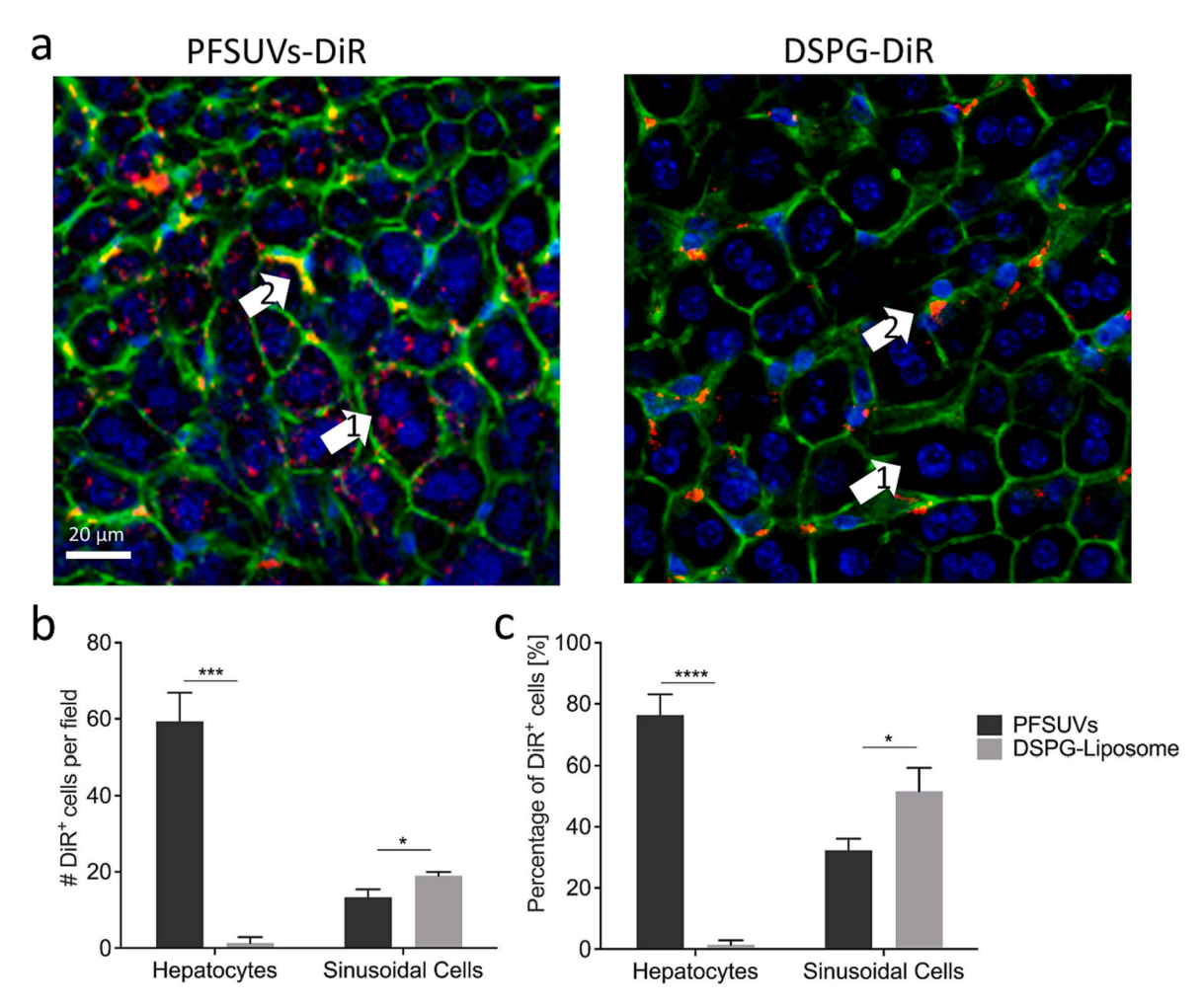


Fig. 4. Intrahepatic distribution of DiR labeled PFSUVs and DSPG-liposomes. Confocal microscopy images of liver sections collected from female CD-1 mice 2 h after injection with DiR labeled particles (red). Sections were stained with DAPI (blue) and Alexa Fluor® 488 Phalloidin (green). Arrows 1 and arrows 2 represent hepatocytes and sinusoidal cells, respectively, identified by their nuclear morphology and phalloidin staining. (b) Total number of DiR-positive hepatocytes and sinusoidal cells per image filed. (c) Percentage of DiR-positive hepatocyte and sinusoidal cells. Comparisons between groups were made unpaired t-test, *: P < 0.05; ***: P < 0.001; ****: P < 0.0001). Data = mean \pm SEM (n = 3). (For interpretation of the references to colour in this figure legend, the reader is referred to the web version of this article.)

and Alexa Fluor® 488-Phalloidin for actin (cell morphology), and imaged by confocal microscopy. As shown in Fig. 4, the cellular and nuclear morphology as well as the outline of the sinusoidal compartment by the Phalloidin staining allowed differentiation of the hepatocytes (indicated by arrow 1) from the sinusoidal Kupffer cells (indicated by arrow 2). PFSUVs and DSPG-liposomes displayed significantly different intrahepatic distribution: most PFSUVs-DiR was found inside the hepatocytes, while DSPG-DiR was exclusively associated with cells in the

sinusoidal compartment. The images were quantified, demonstrating that PFSUVs were detected in 80% of the hepatocytes compared to only 2% of the hepatocytes were stained positive with DSPG-liposomes. In contrast, DSPG-liposomes were found associated with 60% of sinusoidal cells (*i.e.* Kupffer cells) and PFSUVs were detected in only 30% of the sinusoidal cells.

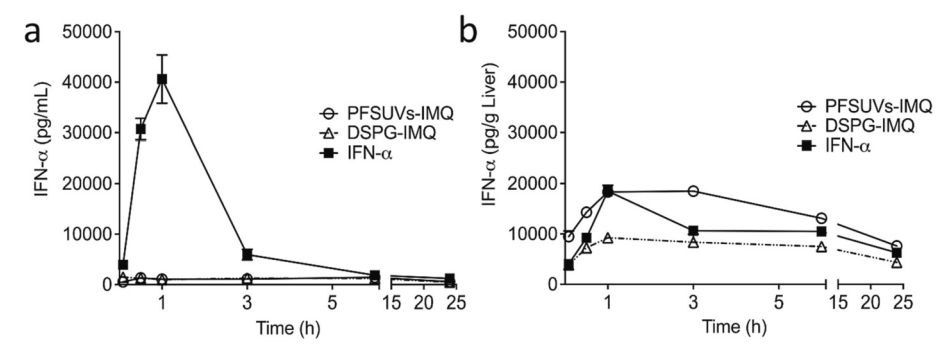


Fig. 5. IFN-α levels in the (a) plasma, and (b) liver after mice treated with PFSUVs-IMQ, DSPG-IMQ (5 mg IMQ/kg), or IFN-α at 1.23 μg (30,000 IU). Data = mean \pm SEM (n=3–5). SEM bars are within some data symbols.

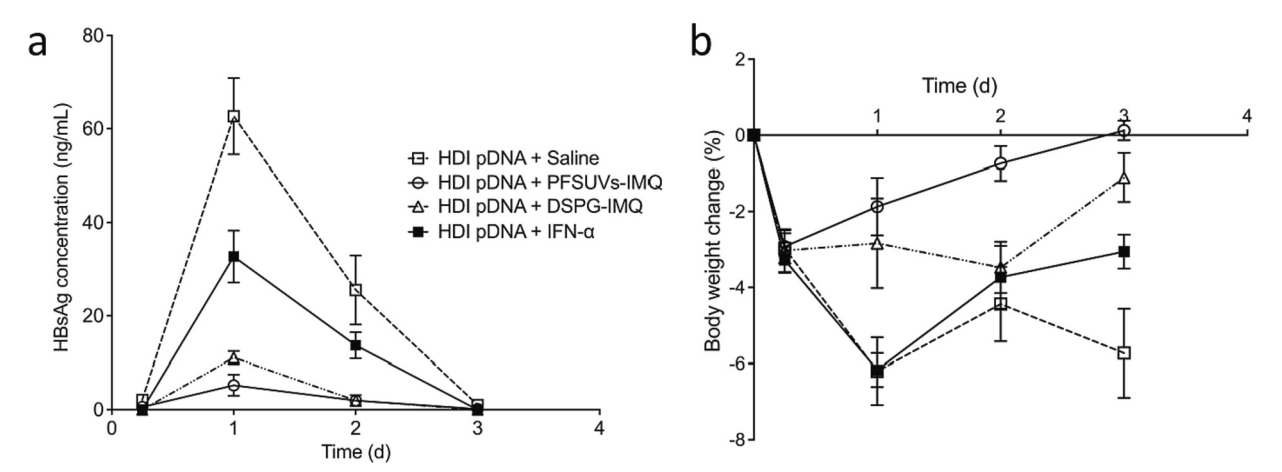


Fig. 6. Therapeutic efficacy of different treatments in experimental HBV model in mice. (a) Plasma HBsAg concentrations and (b) body weight of female CD-1 mice transfected with 10 μg HBsAg pDNA *via* HDI and then treated with saline, PFSUVs-IMQ, DSPG-IMQ (i.v. at 5 mg IMQ/kg) or exogenous IFN- α (s.c. at 1.23 μg or 30,000 IU). Comparisons between groups were made by one-way ANOVA, Data = mean \pm SEM (n = 4–8).

Table 4 Area under the curve analysis of the IFN- α concentrations in Fig. 5. Data = mean \pm SEM (n = 3–5).

	PFSUVs-IMQ	DSPG-IMQ	IFN-α
AUC $_{IFN-\alpha}$ in plasma (ng*h/mL) AUC $_{IFN-\alpha}$ in liver (ng*h/g)	$\begin{array}{c} 5.47 \pm 0.32 \\ 72.75 \pm 1.34 \end{array}$	$5.67 \pm 0.58 \\ 36.52 \pm 0.92$	81.68 ± 1.48 54.01 ± 1.20
AUC _{liver} /AUC _{plasma}	13.29	6.44	0.66

3.5. Cytokine stimulation in the liver

IMQ can activate the interferon regulatory factor 5 (IRF5) pathway upon activating the TLR7, leading to the release of IFN- α , which is a potent antiviral molecule [22,23]. The released IFN- α can further interact with type I interferon receptor 1 (IFNAR1) and activate the IRF9 pathway in parallel with IRF5, resulting in further IFN- α production [24]. After administering PFSUVs-IMQ, DSPG-IMQ or IFN- α to female CD-1 mice, the plasma was isolated and analyzed for IFN- α levels. As presented in Fig. 5a, there was no difference between the two LNP groups in inducing plasma IFN- α levels, which were low (<1000 pg/mL). In contrast, mice treated with exogenous IFN- α exhibited 40-fold increased peak levels of IFN- α in plasma at 1 h compared to the LNP groups. The values of AUC of Fig. 6 are reported in Table 4, wherein the AUC_{plasma} in the IFN- α group was 15-fold higher than the PFSUV-IMQ and DSPG-IMQ groups.

As shown in Fig. 6b, significant IFN- α levels in the liver were detected 5 min after treatment, rapidly reached the peak at 1–3 h, and slowly declined over 24 h for all three groups. Fig. 6b also show that PFSUVs-IMQ was the most effective in producing IFN- α in the liver, followed by IFN- α and DSPG-IMQ. The AUC $_{liver}$ in the PFSUVs-IMQ group was 1.3- and 2-fold higher than that in the IFN- α and DSPG-IMQ groups, respectively.

The AUC_{liver}/AUC_{plasma} (Fig. 5) were 13.29 and 6.44 for the PFSUVs-IMQ and DSPG-IMQ groups, respectively (Table 4), suggesting both LNP formulations selectively induced IFN- α in the liver and minimally provoked systemic response. On the other hand, the AUC_{liver}/AUC_{plasma} in

Table 5 Area under the curve analysis of the HBsAg concentration profiles in Fig. 6a. Data = mean \pm SEM (n = 4–8).

	PFSUVs- IMQ	DSPG-IMQ	IFN-α	Untreated
AUC _{HBsAg} (ng*d/ mL)	5.15 ± 0.62	$\begin{array}{c} 11.25 \pm \\ 0.98 \end{array}$	$51.85 \pm \\1.38$	95.90 ± 1.06

the IFN- α group was 0.66, indicating poor liver selectivity. The results from the IFN- α group were consistent with previous reports [25], and our data imply that the LNP formulations, in particular the hepatocyte-targeting PFSUVs-IMQ, would display enhanced efficacy and reduced systemic toxicity.

3.6. In vivo efficacy

In a cohort study of patients acutely infected with HBV, IFN- α was undetectable in the plasma throughout the duration of viral infection and replication [26]. Recently, the suppression of IFN- α has been linked to the presence of HBsAg in plasma [27]. It was demonstrated that HBsAg inhibited the IRF7 signaling pathway, resulting in IFN-α silencing [28]. Other reports showed that HBV-derived proteins downregulated the expression of IFNAR1 via inhibition of the IRF9 pathway as well as interacted with the IFNAR1 to disturb its binding with IFN- α [29,30]. On the other hand, the resigimod (TLR7/8 agonist) treatment increased the IFN- α and reduced the HBsAg in a HepG2 cell model [6]. Additionally, studies on humanized mice model showed that IFN- α upregulated the transcription of IFN-stimulated genes (ISGs), which in turn inhibited HBV DNA repair from partial dsDNA to covalently closed circular DNA (cccDNA) and its transcription [31,32]. These results suggest that TLR agonists that involve with the IFN pathway via IRF5 upregulation would exhibit anti-HBV activity.

To validate the effect of IMQ, a TLR7 agonist, on reducing HBsAg levels in hepatocytes, we first established an *in vitro* model by transfecting HBsAg pDNA into HepG2 cells. The cells were then treated with IMQ 6 h post transfection and incubated for 3 days. The HBsAg levels in the culture media from the transfected HepG2 cells were significantly reduced by 92% and 88.7% by treatment with IMQ at 0.05 and 0.01 mg IMQ/mL, respectively (supplementary information, Fig. S.2). Our results support that if IMQ could be delivered to the hepatocytes, HBsAg would be decreased, demonstrating therapeutic effect for CHB.

Based on the *in vitro* model and results, we then moved on to *in vivo* studies in mice. We first utilized the hydrodynamic injection (HDI) method to transfect HBsAg pDNA into the hepatocytes in mice. HDI is a well-established technique that has been shown to effectively deliver pDNA to the hepatocytes by rapidly injecting a large volume of pDNA containing saline into mice through the tail vein [16]. The mice were then treated with saline, exogenous IFN- α , PFSUVs-IMQ or DSPG-IMQ in 6 h. Plasma was collected from the mice at 6 h (right before drug treatment), 1 d, 2 d and 3 d after HDI and measured for HBsAg by ELISA. As reported in Fig. 6a, the plasma HBsAg concentration in mice peaked 1d after HDI and the expression was only transient for 2–3 days. However, this model allowed us to robustly compare short-term efficacy of

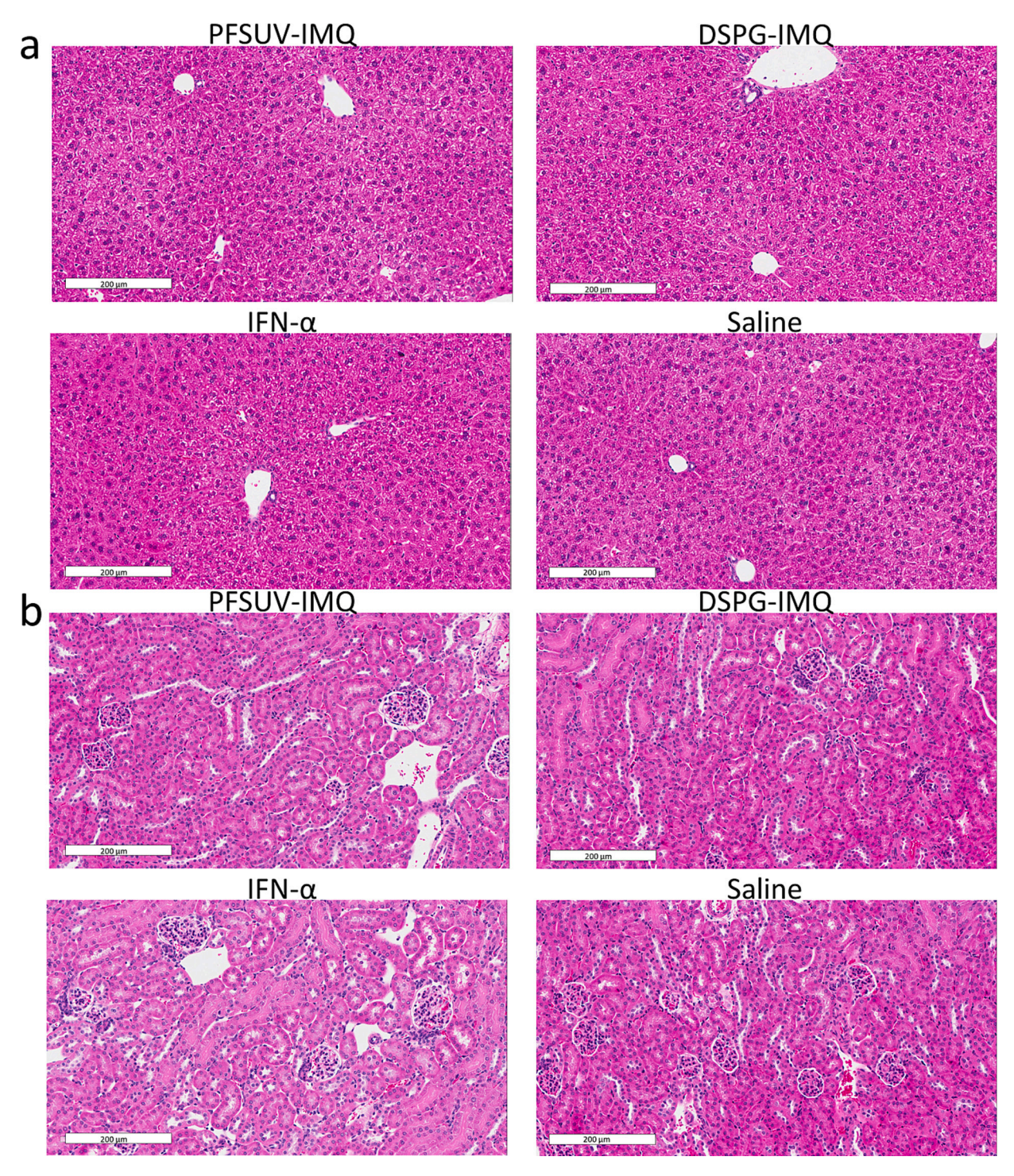


Fig. 7. Representative images of haematoxylin and eosin-stained sections of mouse (a) liver (b) kidney (c) heart (d) lung and (e) spleen at 3 days post treatment with saline, PFSUVs-IMQ, DSPG-IMQ (at 5 mg IMQ/kg), or exogenous IFN- α (s.c. at 1.23 μ g or 30,000 IU). Scale bar represents 200 μ m.

treatments. As shown in Fig. 6a, PFSUVs-IMQ displayed the highest efficacy against HBsAg, followed by DSPG-IMQ, and then IFN- α . The AUC_{HBsAg} in the PFSUVs-IMQ group was 2-, 10-, and \sim 20-fold reduced compared to the treatments with DSPG-IMQ, IFN- α , and saline, respectively (Table 5). The superior efficacy of PFSUVs-IMQ is consistent with its enhanced liver IFN- α inducing activity that can be attributed to its efficient targeting to the hepatocytes. Although DSPG-IMQ induced lower liver IFN- α production compared to exogenous IFN- α , the AUC_{HBsAg} in the DSPG-IMQ group was \sim 5-fold reduced compared to the

IFN- α group. This result is unexpected and requires further investigation. A plausible explanation is that DSPG-IMQ was more effective in activating the Kupffer cells through the targeted delivery compared to exogenously delivered IFN- α , and activated Kupffer cells have been shown to directly transport antiviral molecules, such as APOBEC3G, to the hepatocytes, decreasing the HBsAg expression [33,34].

It has been demonstrated that expression of HBsAg in the hepatocytes induced endoplasmic reticulum stress, resulting in unfolded protein response (UPR) that contributed to the liver pathogenesis during the

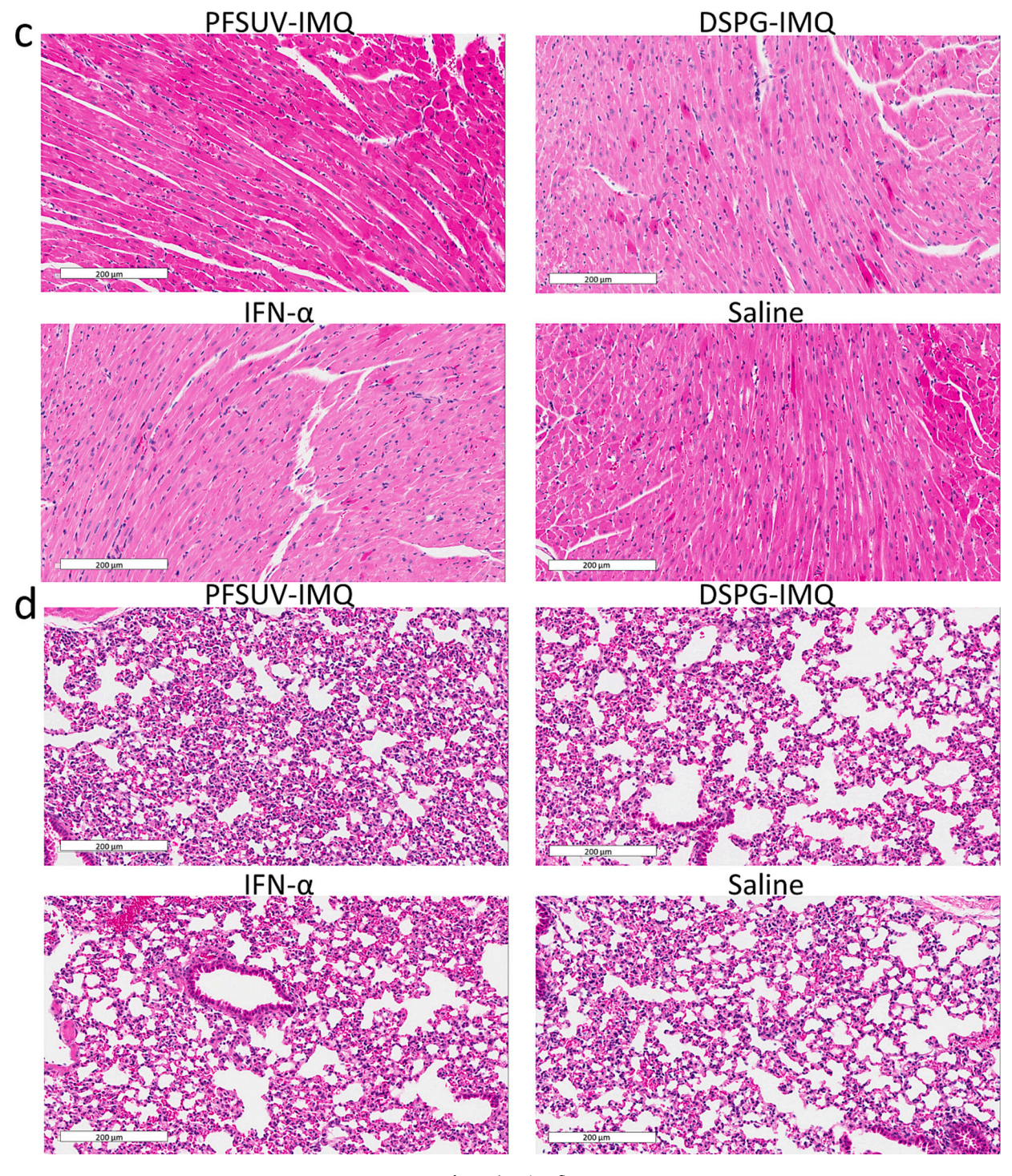


Fig. 7. (continued).

HBV infection [35]. Therefore, health of the mice, such as body weight, could be affected by HBsAg transfection, and can be used as a phenotypic marker for comparing the treatment efficacy. As shown in Fig. 6b, 6 h post HDI of HBsAg pDNA, all mice lost $\sim\!\!3\%$ body weight, possibly due to the stress from the HDI procedure. After that, mice treated with PFSUVs-IMQ rapidly and fully regained their body weight in 3 days. The DSPG-IMQ group maintained their body weight from 6 h to 2 days, and by day 3, only 1% body weight loss was measured. IFN- α treated mice, however, continued to lose their weight after 6 h until day 1 ($\sim\!\!6\%$), followed by gradual rebound to 4% loss on day 3. The saline treated group showed continuous weight loss after HDI, reaching 6% loss on day

1 and did not regain any weight until day 3. The body weight data are consistent with the plasma HBsAg results, showing that PFSUVs-IMQ exerted the best therapeutic efficacy in this model and improved the general health of mice, followed by DSPG-IMQ and then IFN- α .

We acknowledge that the model we used in this work is an experimental model instead of a real disease model of chronic hepatitis B (CHB), which is challenging to access. However, this experimental model recapitulates outcomes of IFN- α therapy in HBV-infected hepatocytes, allowing us to obtain proof-of-principle results to demonstrate the therapeutic potential of IMQ-PFSUVs. It has been shown by Belloni et al. [32] in a humanized HBV-mouse model, that IFN- α inhibited

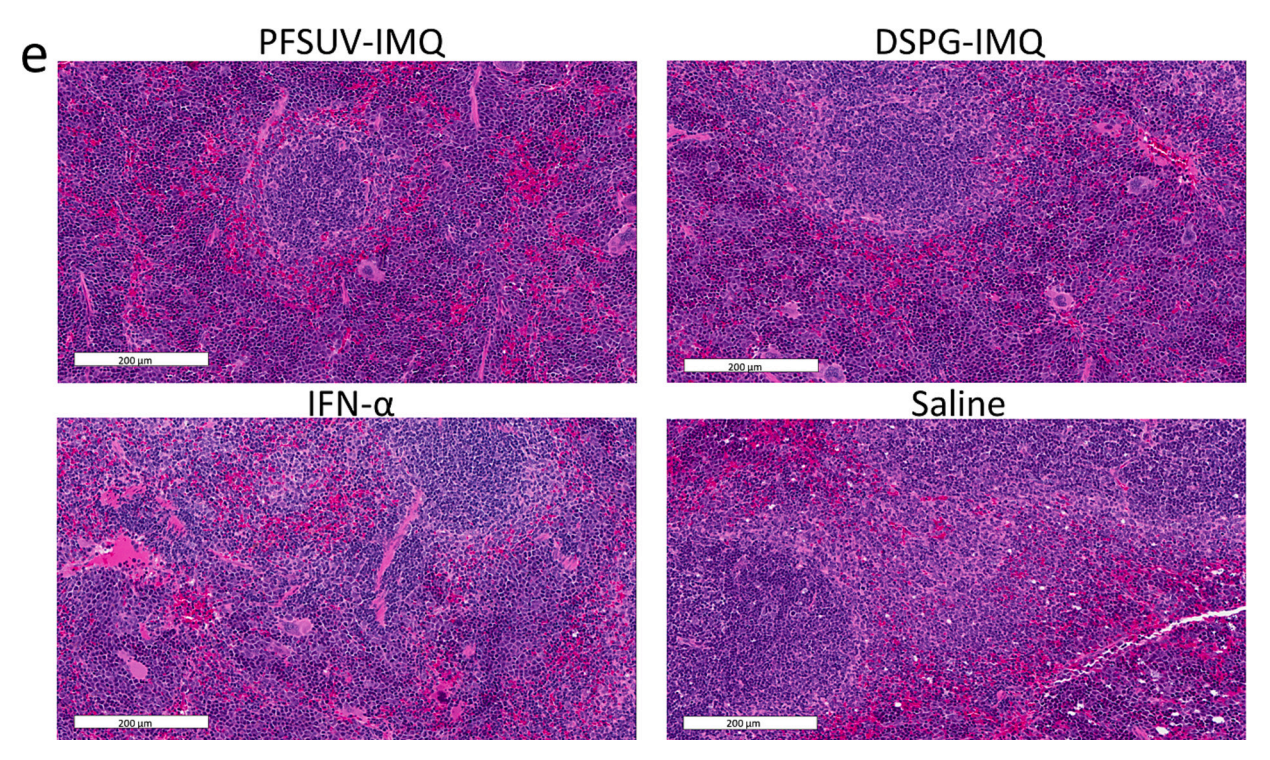


Fig. 7. (continued).

Table 6 Liver and blood biomarker values in mice treated with PFSUVs-IMQ, DSPG-IMQ, IFN- α or saline compared to normal values. Data = mean \pm SEM (n = 4).

Test	PFSUVs- IMQ	DSPG- IMQ	IFN-α	Saline	Normal
Liver					
ALT (U/L)	26.00 \pm	33.25 \pm	48.75 \pm	25.80 \pm	41.63 \pm
	3.37	7.12	15.69	3.78	1.82
AST (U/L)	98.75 \pm	133.67 \pm	60.00 \pm	113.20 \pm	82.8 \pm
	26.42	36.75	5.65	31.21	5.23
Blood					
RBC (x10 ¹² /L)	7.00 \pm	6.98 \pm	6.55 \pm	6.74 \pm	8.77 \pm
	0.28	0.15	0.29	0.32	0.15
Hematocrit	0.37 \pm	0.39 \pm	0.34 \pm	0.36 \pm	$0.49 \pm$
(L/L)	0.01	0.02	0.01	0.01	0.01
Hemoglobin	107.50 \pm	111.25 \pm	101.00	105.00 \pm	$145~\pm$
(g/L)	4.63	3.40	\pm 3.72	3.66	2.69
MCV (fL) †	52.78 \pm	55.83 \pm	52.40 \pm	54.04 \pm	56.39 \pm
	1.49	1.52	0.96	0.48	0.49
MCH (pg) †	15.40 \pm	15.95 \pm	15.43 \pm	15.62 \pm	$16.59 \pm$
	0.04	0.18	0.12	0.25	0.14
MCHC (g/L) †	292.63 \pm	285.93 \pm	294.88	288.92 \pm	295.2 \pm
	8.25	6.23	\pm 4.35	4.62	3.47
RDW (%) †	19.95 \pm	$21.50\ \pm$	21.08 \pm	20.60 \pm	16.62 \pm
	0.69	1.11	0.89	0.96	0.14

 \dagger MCV - Mean Corpuscular Volume, MCH mean corpuscular hemoglobin, MCHC - mean corpuscular hemoglobin concentration, RDW - Red cell distribution width.

replication and transcription of viral genes including HBsAg, leading to reduced plasma HBsAg. Based on this prior study, we first confirmed in a cell culture model that when IMQ was delivered to HepG2 cells that were transfected with HBsAg pDNA, release of HBsAg was suppressed (supplementary Fig. S.2). In the experimental animal model, when IMQ was targeted to the HBsAg pDNA-transfected hepatocytes by PFSUVs, IFN- α was locally induced and the expression of HBsAg was decreased. In these experimental models, only HBsAg was introduced instead of the whole virus, permitting robust analysis of IFN- α therapies since HBsAg

was released into the culture medium or plasma from the transfected cells and could be quantified by ELISA. Nevertheless, IMQ-PFSUVs must be tested in a HBV-infected animal model to conclude the therapeutic effect, which will be pursued in the future through collaborations.

We also performed detailed toxicology studies in these experimental HBV mice by examining their serum liver enzymes, blood chemistry and tissue histology on day 3. The results in Fig. 6 suggest that mice treated with IFN-α would display increased toxicity from the treatment compared to others, as the systemic IFN- α levels were 15-fold higher. However, there were no toxicities for all three treatments (Fig. 7 and Table 6), and the toxicology data were comparable among the groups, including the saline group and normal ranges reported in the literature. The data also support that even both the LNP formulations targeted a large dose to the liver, the tissue toxicity was not significant. Although IFN- α did not show any toxicity at this dose in this animal model, its nonspecific delivery evidenced in Fig. 5 and Table 4 suggests that this treatment would induce systemic toxicity at a higher or therapeutic dose. On the other hand, the liver-targeted LNP therapeutics, in particular the hepatocyte-targeted PFSUVs-IMQ, are expected to display enhanced therapy and decreased side effects.

Overall, the *in vivo* study demonstrated that the hepatocyte-targeted PFSUVs-IMQ was safe and superior to the standard IFN- α therapy and the Kupffer cell-targeted DSPG-IMQ in suppressing HBsAg.

4. Conclusion

This study demonstrated that PFSUVs were able to encapsulate IMQ and stably retain it in the presence of serum. PFSUVs selectively delivered IMQ to the hepatocytes to locally increase IFN- α levels in the liver in mice and subsequently reduced the plasma HBsAg, demonstrating its potential for treating CHB. IMQ loaded in DSPG-liposomes that targeted the Kupffer cells was inferior to PFSUVs-IMQ in provoking IFN- α release in the liver and reducing plasma HBsAg. The standard IFN- α therapy given by s.c. injection induced global IFN- α response, while the effect in suppressing plasma HBsAg was lower compared to the above LNP formulations. Our results suggest that the hepatocyte-targeted PFSUVs-IMQ may provide safe and enhanced therapy for CHB compared to

standard IFN-α.

CRediT authorship contribution statement

Nojoud AL Fayez: Investigation, Methodology, Formal analysis, Visualization, Writing – original draft. Elham Rouhollahi: Investigation. Chun Yat Ong: Investigation. Jiamin Wu: Investigation. Anne Nguyen: Investigation. Roland Böttger: Investigation. Pieter R. Cullis: Project administration, Supervision. Dominik Witzigmann: Investigation, Visualization. Shyh-Dar Li: Conceptualization, Funding acquisition, Supervision, Writing – review & editing.

Acknowledgements

This work was supported by the Canadian Institutes of Health Research (CIHR, grant no. PJT-168861), the Natural Science and Engineering Research Council in Canada (NSERC, grant no. RGPIN-2017-03787), the Canada Foundation for Innovation (CFI, grant no. 35816), and the Mitacs Accelerate grant (no. IT13402) sponsored by Mitacs and Precision Nanosystems Inc., Canada (grant no. 18004). S.D.L. received the Angiotech Professorship in Drug Delivery. N.A.F. received a full Ph. D. scholarship from King Abdulaziz City for Science and Technology (KACST) in Saudi Arabia. R.B. is supported by a postdoctoral fellowship from the German Research Foundation (DFG; grant no. 423802991). D. W. acknowledges the support by the Swiss National Science Foundation Postdoc Mobility Fellowship (no. 183923). We acknowledge Dr. Natalie Strynadka and Dr. Florian Rossmann from the UBC High Resolution Macromolecular Cryo-Electron Microscopy facility for supporting the cryo-TEM imaging.

Appendix A. Supplementary data

Supplementary data to this article can be found online at https://doi.org/10.1016/j.jconrel.2022.08.058.

References

- [1] R. Williams, Global challenges in liver disease, Hepatology. 44 (2006) 521–526, https://doi.org/10.1002/HEP.21347.
- [2] World Health Organization, Global Health Sector Strategy on Viral Hepatitis 2016-2021 (n.d.), https://www.who.int/publications/i/item/WHO-HIV-2016.06, 2022 (accessed February 17, 2022).
- [3] A.S.J. Woo, R. Kwok, T. Ahmed, Alpha-interferon treatment in hepatitis B, Ann. Transl. Med. 5 (2017), https://doi.org/10.21037/atm.2017.03.69.
- [4] G.M. Barton, R. Medzhitov, Toll-like receptor signaling pathways, Science 300 (2003) 1524–1525, https://doi.org/10.1126/SCIENCE.1085536.
- [5] T. Kawasaki, T. Kawai, Toll-like receptor signaling pathways, Front. Immunol. 5 (2014) 461, https://doi.org/10.3389/FIMMU.2014.00461/BIBTEX.
- [6] C. Xia, M. Lu, Z. Zhang, Z. Meng, Z. Zhang, C. Shi, TLRs antiviral effect on hepatitis B virus in HepG2 cells, J. Appl. Microbiol. 105 (2008) 1720–1727, https://doi.org/ 10.1111/J.1365-2672.2008.03896.X.
- [7] D.H. Dockrell, G.R. Kinghorn, Imiquimod and resiquimod as novel immunomodulators, J. Antimicrob. Chemother. 48 (2001) 751–755, https://doi. org/10.1093/JAC/48.6.751.
- [8] E.W.M. Van Etten, M. Otte-lambillion, W. Van Vianen, M.T.T. Kate, I.A.J. M. Bakker-woudenberg, Biodistribution of liposomal amphotericin B (AmBisome) and amphotericin B-desoxycholate (Fungizone) in uninfected immunocompetent mice and leucopenic mice infected with Candida albicans, J. Antimicrob. Chemother. 35 (1995) 509–519, https://doi.org/10.1093/JAC/35.4.509.
- [9] W. Zhang, R. Böttger, Z. Qin, J.A. Kulkarni, J. Vogler, P.R. Cullis, S. Li, Phospholipid-Free Small Unilamellar Vesicles for Drug Targeting to Cells in the Liver 1901782, 2019, pp. 1–12, https://doi.org/10.1002/smll.201901782.
- [10] J. Vogler, R. Böttger, N.A.L. Fayez, W. Zhang, Z. Qin, L. Hohenwarter, P.-H. Chao, E. Rouhollahi, N. Bilal, N. Chen, B. Lee, C. Chen, B. Wilkinson, T.J. Kieffer, J. A. Kulkarni, P.R. Cullis, D. Witzigmann, S.-D. Li, Altering the intra-liver distribution of phospholipid-free small unilamellar vesicles using temperature-dependent size-tunability, J. Control. Release 333 (2021) 151–161, https://doi.org/10.1016/j.jconrel.2021.03.025.
- [11] N. Al Fayez, R. Böttger, E. Rouhollahi, P.R. Cullis, D. Witzigmann, S.D. Li, Improved liver delivery of Primaquine by phospholipid-free small unilamellar vesicles with reduced hemolytic toxicity, Mol. Pharm. (2021), https://doi.org/ 10.1021/acs.molpharmaceut.1c00520.
- [12] E. Hanna, R. Abadi, O. Abbas, Imiquimod in dermatology: an overview, Int. J. Dermatol. 55 (2016) 831–844, https://doi.org/10.1111/JJD.13235.

- [13] D. Das, I. Sengupta, N. Sarkar, A. Pal, D. Saha, M. Bandopadhyay, C. Das, J. Narayan, S.P. Singh, S. Chakrabarti, R. Chakravarty, Anti-hepatitis B virus (HBV) response of imiquimod based toll like receptor 7 ligand in hbv-positive human hepatocelluar carcinoma cell line, BMC Infect. Dis. 17 (2017) 1–12, https://doi. org/10.1186/S12879-017-2189-Z/FIGURES/6.
- [14] P.J. Pockros, D. Guyader, H. Patton, M.J. Tong, T. Wright, J.G. Mchutchison, T.-C. Meng, Oral Resiquimod in Chronic HCV Infection: Safety and Efficacy in 2 Placebo-Controlled, Double-Blind Phase IIa Studies q,qq (n.d.), 2022, https://doi.org/10.1016/j.jhep.2007.02.025.
- [15] G. Pauli, W.L. Tang, S.D. Li, Development and characterization of the solventassisted active loading technology (SALT) for liposomal loading of poorly watersoluble compounds, Pharmaceutics. 11 (2019) 465, https://doi.org/10.3390/ pharmaceutics11090465.
- [16] B. Bonamassa, H. Li, D. Liu, Hydrodynamic Gene Delivery and Its Applications in Pharmaceutical Research (n.d.), 2022, https://doi.org/10.1007/s11095-010-0338-
- [17] B. Cacopardo, F. Benanti, M.R. Pinzone, G. Nunnari, Rheumatoid arthritis following PEG-interferon-alfa-2a plus ribavirin treatment for chronic hepatitis C: a case report and review of the literature, BMC Res. Notes 6 (2013) 1–4, https://doi. org/10.1186/1756-0500-6-437/TABLES/2.
- [18] W. Zhao, F. Ji, S. Yu, Z. Li, H. Deng, Dilated cardiomyopathy and hypothyroidism associated with pegylated interferon and ribavirin treatment for chronic hepatitis C: case report and literature review, Brazilian, J. Infect. Dis. 18 (2014) 110–113, https://doi.org/10.1016/J.BJID.2013.05.014.
- [19] W.L. Tang, W.H. Tang, A. Szeitz, J. Kulkarni, P. Cullis, S.D. Li, Systemic study of solvent-assisted active loading of gambogic acid into liposomes and its formulation optimization for improved delivery, Biomaterials. 166 (2018) 13–26, https://doi. org/10.1016/j.biomaterials.2018.03.004.
- [20] W.L. Tang, W.H. Tang, W.C. Chen, C. Diako, C.F. Ross, S.D. Li, Development of a rapidly dissolvable oral pediatric formulation for mefloquine using liposomes, Mol. Pharm. 14 (2017) 1969–1979, https://doi.org/10.1021/acs. molpharmaceut.7b00077.
- [21] C.I. Colino, J.M. Lanao, C. Gutierrez-Millan, Targeting of hepatic macrophages by therapeutic nanoparticles, Front. Immunol. 11 (2020) 218, https://doi.org/ 10.3389/FIMMU.2020.00218.
- [22] M.V. Dahl, Imiquimod: a cytokine inducer, J. Am. Acad. Dermatol. 47 (2002) S205–S208, https://doi.org/10.1067/MJD.2002.126586.
- [23] A. Schoenemeyer, B.J. Barnes, M.E. Mancl, E. Latz, N. Goutagny, P.M. Pitha, K. A. Fitzgerald, D.T. Golenbock, The interferon regulatory factor, IRF5, is a central mediator of toll-like receptor 7 signaling *, J. Biol. Chem. 280 (2005) 17005–17012, https://doi.org/10.1074/JBC.M412584200.
- [24] C.A. Jefferies, Regulating IRFs in IFN driven disease, Front. Immunol. 10 (2019) 325. https://doi.org/10.3389/FIMMU.2019.00325/BIBTEX.
- [25] D. Rycroft, J. Sosabowski, E. Coulstock, M. Davies, J. Morrey, S. Friel, F. Kelly, R. Hamatake, M. Ovečka, R. Prince, L. Goodall, A. Sepp, A. Walker, Pharmacokinetic Characteristics, Pharmacodynamic Effect and In Vivo Antiviral Efficacy of Liver-Targeted Interferon Alpha, 2015, https://doi.org/10.1371/ journal.pone.0117847.
- [26] C. Dunn, D. Peppa, P. Khanna, G. Nebbia, M. Jones, N. Brendish, R.M. Lascar, D. Brown, R.J. Gilson, R.J. Tedder, G.M. Dusheiko, M. Jacobs, P. Klenerman, M. K. Maini, Temporal analysis of early immune responses in patients with acute hepatitis b virus infection, Gastroenterology. 137 (2009) 1289–1300, https://doi.org/10.1053/J.GASTRO.2009.06.054/ATTACHMENT/635BC71B-FFCF-4264-8FA2-4RA95282CB92/MMC1.PDF.
- [27] A.M. Woltman, M.L.O. den Brouw, P.J. Biesta, C.C. Shi, H.L.A. Janssen, Hepatitis B virus lacks immune activating capacity, but actively inhibits plasmacytoid dendritic cell function, PLoS One 6 (2011) 15324, https://doi.org/10.1371/ JOURNAL PONE.0015324.
- [28] Y. Xu, Y. Hu, B. Shi, X. Zhang, J. Wang, Z. Zhang, F. Shen, Q. Zhang, S. Sun, Z. Yuan, HBsAg inhibits TLR9-mediated activation and IFN-α production in plasmacytoid dendritic cells, Mol. Immunol. 46 (2009) 2640–2646, https://doi.org/10.1016/J.MOLJMM.2009.04.031.
- [29] J. Chen, W. Xu, Y. Chen, X. Xie, Y. Zhang, C. Ma, Q. Yang, Y. Han, C. Zhu, Y. Xiong, K. Wu, F. Liu, Y. Liu, J. Wu, Matrix metalloproteinase 9 facilitates hepatitis B virus replication through binding with type I interferon (IFN) receptor 1 to repress IFN/JAK/STAT signaling, J. Virol. 91 (2017) 1824–1840, https://doi.org/10.1128/JVI.01824-16.
- [30] L. Bai, W. Zhang, L. Tan, H. Yang, M. Ge, C. Zhu, R. Zhang, Y. Cao, J. Chen, Z. Luo, W. Ho, F. Liu, K. Wu, J. Wu, Hepatitis B virus hijacks CTHRC1 to evade host immunity and maintain replication, J. Mol. Cell Biol. 7 (2015) 543–556, https://doi.org/10.1093/JMCB/MJV048.
- [31] C. Boni, A. Vecchi, M. Rossi, D. Laccabue, T. Giuberti, A. Alfieri, P. Lampertico, G. Grossi, F. Facchetti, M.R. Brunetto, B. Coco, D. Cavallone, A. Mangia, R. Santoro, V. Piazzolla, A. Lau, A. Gaggar, G.M. Subramanian, C. Ferrari, Basic And Translational-Liver TLR7 Agonist Increases Responses of Hepatitis B Virus-Specific T Cells and Natural Killer Cells in Patients with Chronic Hepatitis B Treated with Nucleos(T)Ide Analogues, 2018, https://doi.org/10.1053/j.gastro.2018.01.030.
- [32] L. Belloni, L. Allweiss, F. Guerrieri, N. Pediconi, T. Volz, T. Pollicino, J. Petersen, G. Raimondo, M. Dandri, M. Levrero, IFN-α inhibits HBV transcription and replication in cell culture and in humanized mice by targeting the epigenetic regulation of the nuclear cccDNA minichromosome, J. Clin. Invest. 122 (2012) 529–537, https://doi.org/10.1172//CI58847.

- [33] L. Yc, H. Yh, Z. Zm, T. Yj, W. Bj, Y. Yang, Z. Xp Lu, The Levels of Intracellular Core-Associated HBV DNA and Extracellular Production of HBsAg and HBeAg. http ://www.wjgnet.com/1007-9327/12/4492.asp, 2006.
- [34] J. Li, K. Liu, Y. Liu, Y. Xu, F. Zhang, H. Yang, J. Liu, T. Pan, J. Chen, M. Wu, X. Zhou, Z. Yuan, Exosomes mediate the cell-to-cell transmission of IFN- α -induced
- antiviral activity, Nat. Immunol. 148 (14) (2013) 793–803, https://doi.org/
- [35] Y. Li, Y. Xia, X. Cheng, D.E. Kleiner, S.M. Hewitt, J. Sproch, T. Li, H. Zhuang, T. Jake Liang, Hepatitis B surface antigen activates unfolded protein response in forming ground glass hepatocytes of chronic hepatitis B, Viruses 11 (2019) 386, https://doi.org/10.3390/V11040386.